ELSEVIER

Surface Science 304 (1994) 185–190

surface science

Strong coupling of Rayleigh phonons to charge density waves in 1T-TaS_2

G. Benedek *,[1], G. Brusdeylins, F. Hofmann, P. Ruggerone, J.P. Toennies, R. Vollmer [2]

Max-Planck-Institut für Strömungsforschung, Bunsenstrasse 10, D-37073 Göttingen, Germany

J.G. Skofronick

Department of Physics, Florida State University, Tallahassee, FL 32306, USA

(Received 14 October 1993; accepted for publication 10 November 1993)

Abstract

The dispersion curves of charge density wave (CDW)-induced phonons have been measured in 1T-TaS_2 by inelastic He atom scattering along both crystallographic and CDW symmetry directions. Evidence is given for a strong coupling of the CDW to Rayleigh waves, i.e. to quasi-transverse acoustic modes. A pseudocharge model analysis of lattice dynamics accounts for the CDW-induced splitting of the Raman-active modes originated from the folding of transverse acoustic modes.

The nature of the electron–phonon coupling that drives charge density waves (CDWs) in low-dimensional systems has attracted much attention in recent years [1,2]. In spite of such interest, the present knowledge of the phonon spectrum in CDW low-dimensional systems and the role of electron–phonon coupling is rather limited, primarily because of the intrinsic difficulty in obtaining thick stacking-fault-free samples suitable for neutron spectroscopy [3–5].

In this work we have investigated the phonon dispersion curves of the basal (001) surface of TaS_2 (1T polytype with $CdCl_2$ structure) at 120 K by means of inelastic He atom scattering (HAS). At this temperature the crystal has a commensurate $\sqrt{13} \times \sqrt{13}$ CDW whose symmetry axes are rotated by 13.9° with respect to the crystallographic axes ($1T_3$ phase) [6]. The unit cell is shown in Fig. 1a for the Ta ion sheet. We have observed several transverse branches associated with different reciprocal vectors $\boldsymbol{g}$ of the CDW superstructure and originating from the folding of the Rayleigh wave branch induced by the CDW. The inelastic HAS technique, unlike neutron spectroscopy, is only sensitive to the surface and is therefore suitable for extremely thin crystals. Furthermore, inelastic HAS probes exclusively

* Corresponding author.

[1] Permanent address: Dipartimento di Fisica dell'Università di Milano, via Celoria 16, 20133 Milano, Italy.

[2] Present address: Max-Planck-Institut für Mikrostrukturphysik, Weinberg 2, D-06120 Halle/Saale, Germany.

SSDI 0039-6028(94)E0928-N

the part of the surface electron density that is modulated during the vibrational motion, i.e. the density of electrons whose energy is close to the Fermi surface [7]. The present observation of folded Rayleigh modes provides the first evidence that transverse polarized modes are able to modulate the CDW electron density.

It is commonly accepted that longitudinal acoustic (LA) modes are involved in the electron–phonon interaction at the Fermi surface [1], as suggested by the fact that Kohn anomalies are mostly seen in longitudinal branches [4,5] and CDW-induced distortions are mostly longitudinal in the basal plane [8]. The available experimental information on bulk phonon dispersion curves of 1T-TaS_2, as obtained from inelastic neutron scattering by Ziebeck et al. [3], is restricted to room temperature ($1T_2$ phase) and only the acoustic branches along the c-axis and the LA and TA_1 branches (the latter polarized nearly parallel to the c-axis) along the Σ direction [100] could be measured. These authors could note, however, that the Kohn anomaly in the LA branch falls in a region where LA and TA modes are strongly hybridized. Furthermore, HAS data [9,10] and scanning tunnelling microscopy [11] demonstrate that a large surface corrugation is induced by the CDW in 1T-TaS_2. Thus also inelastic processes associated with the CDW g-vectors are expected to be observed by HAS with comparatively large intensity. Indeed, the present results provide evidence for a very strong coupling of transverse modes to the CDW, which leads to a very large inelastic He scattering intensity from the CDW-induced phonons. It may be argued that the present unusual observation is a special surface effect, since the Rayleigh waves are usually elliptically polarized. We note, however, that in highly anisotropic layered crystals the Rayleigh wave is in fact extremely close to the TA edge and has an

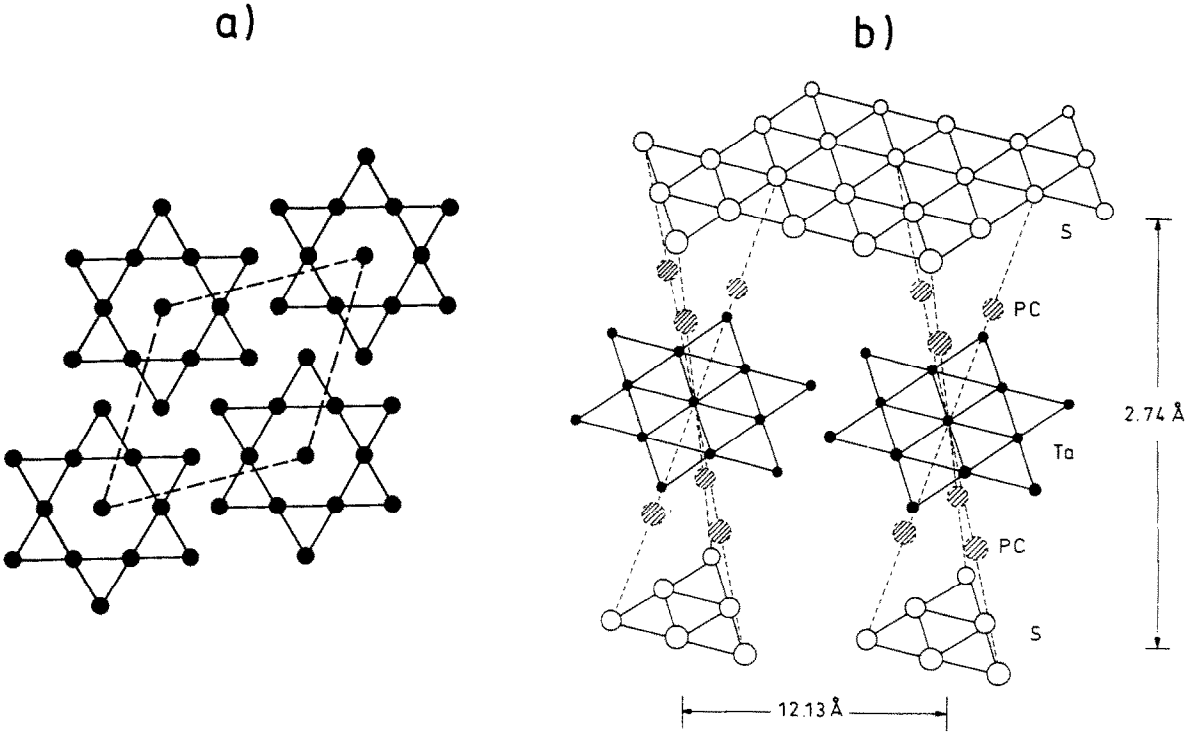

Fig. 1. (a) The sheet of Ta ions in 1T-TaS_2 showing the unit cell (dashed line) in the presence of the commensurate $\sqrt{13} \times \sqrt{13}$ charge density wave ($1T_3$ phase). (b) Location of the pseudocharges (PC) between sheets of sulphur (S) and tantalium ions. An octahedral cage of sulphur ions encloses one Ta ion; in the pseudocharge model the Ta ions at the David star centres are surrounded by six pseudocharges.

almost perfect shear vertical polarization [12]. This was experimentally confirmed in 2H-$TaSe_2$, for temperatures away from the CDW onset temperature [13], as is the case for the present experiments.

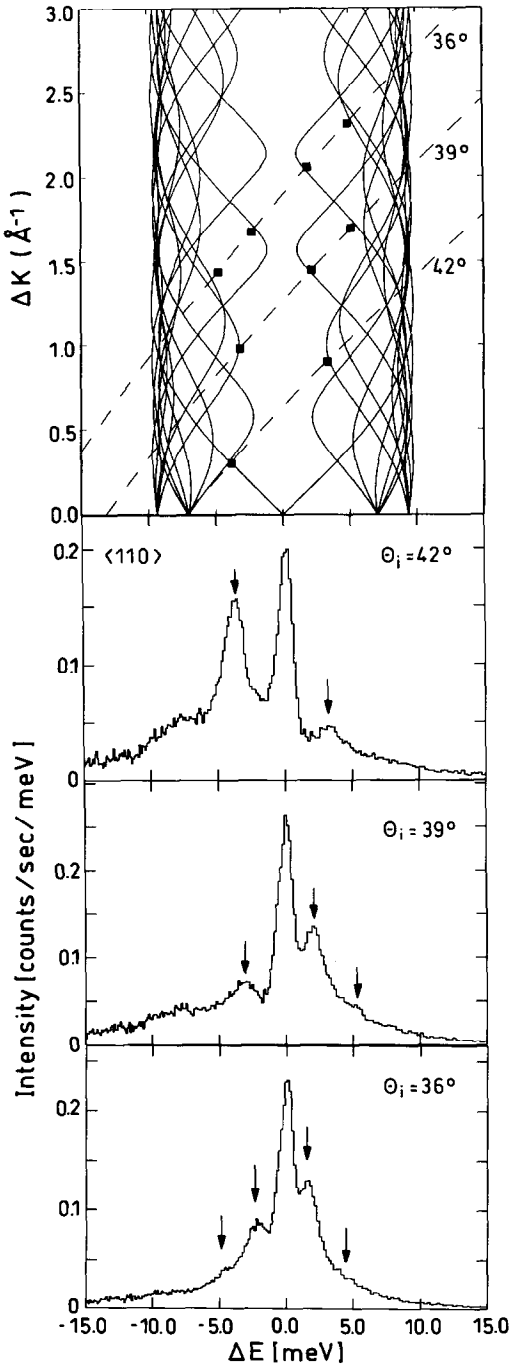

The crystal was inserted into the scattering chamber and baked in the usual way [10]. The single crystal was then cleaved in situ. During the measurements the crystal was periodically heated to 450 K for approximately 10 h to ensure a clean surface. LEED and He atom scattering angular distribution measurements were performed to check the quality of the surface [10]. The scattering apparatus was the same as that used in a previous study of a layered crystal [13]. The supersonic helium beam is produced in a high-pressure nozzle (10 μm diameter) which can be heated to 380 K and cooled to 55 K by a closed-cycle refrigerator. In this way, beam energies between 12 meV ($k_i = 4.8$ Å^{-1}) and 82 meV ($k_i = 12.6$ Å^{-1}) were available. In our measurements we used a helium beam with an incident energy of $E_i = 38.7$ meV ($k_i = 5.94$ Å^{-1}). Time-of-flight HAS spectra were measured for different incident angles θ_i and at a surface temperature $T_s =$ 120 K along the symmetry directions ⟨100⟩ and ⟨110⟩ of the normal phase and the CDW direction (R13.9°). Three examples are shown in Fig. 2 for the ⟨110⟩ direction for $\theta_i = 36°$, 39° and 42°. Besides the elastic diffuse peak various phonon structures are visible on both the creation ($\Delta E <$ 0) and annihilation side ($\Delta E > 0$). The corresponding phonon energies are plotted as a function of the parallel wavevector along the respective scan curves (broken lines, Fig. 2 (top); see also Ref. [10]).

A simple analysis based on a single sinusoidal dispersion relation as folded by the CDW superstructure and with an initial slope given by the transverse wave velocity $v_T = 1656$ m/s [3] (full

Fig. 2. *Bottom*: Inelastic He atom scattering spectra in the ⟨110⟩ direction of $TaS_2(001)$ for three different incidence angles θ_i and incident energy of 38.7 meV. The phonon structures are marked by arrows. *Top*: Phonon peak positions are plotted (black squares) as a function of the transferred parallel wavevector on the scan (energy momentum conservation) curves (broken lines) for the corresponding incidence angles. The fitting curves originate from the folding of one single sinusoidal dispersion produced by the $\sqrt{13} \times \sqrt{13}$ CDW superstructure.

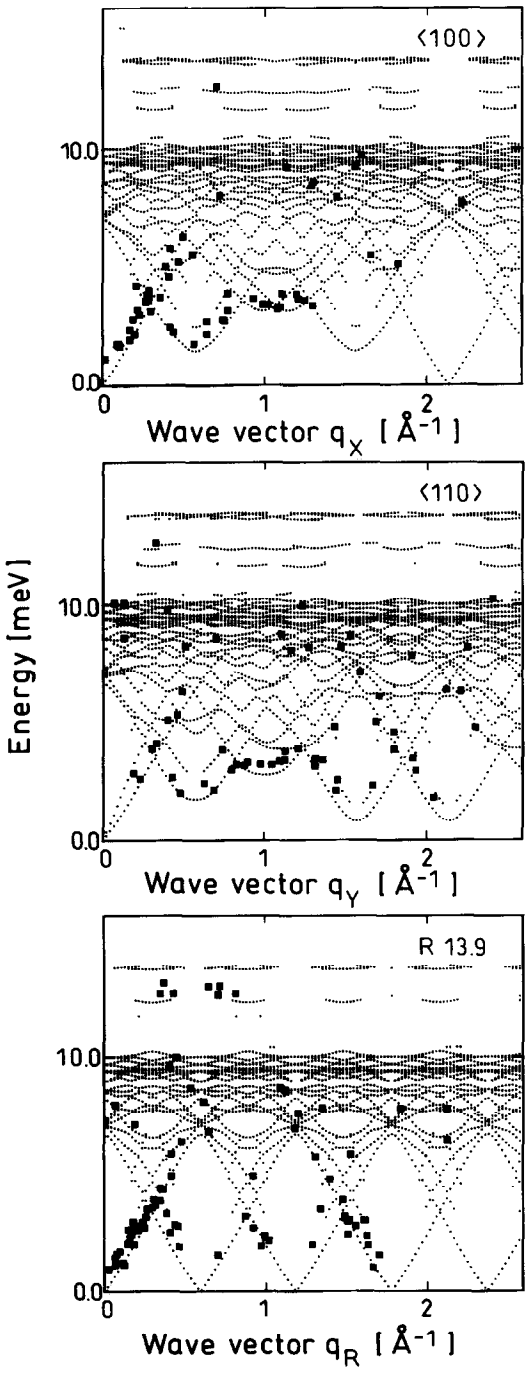

Fig. 3. Full sets of inelastic HAS data along the crystallographic symmetry directions and the CDW symmetry direction R13.9° and calculated phonon dispersion curves (dotted lines) in the acoustic region of 1T-TaS_2 for z-polarized sulphur displacements larger than a given threshold.

lines in Fig. 2 (top)) shows that most of the measured points belong to folded branches, i.e. to Umklapp processes with g-vectors of the commensurate $\sqrt{13} \times \sqrt{13}$ CDW superstructure. Thus they are associated with CDW-induced transverse phonons. As compared to a normal process (e.g. the peak at -4 meV for $\theta = 42°$), the Umklapp peaks, although generally smaller, retain an appreciable intensity up to fairly large g-vectors. Phonons associated with practically all the 13 different g-vectors of the CDW contained in the crystallographic Brillouin zone are observed along the three investigated directions, as shown by the full set of measured points displayed in Fig. 3. Along the CDW direction (R13.9°), fairly sharp peaks are also found around -13 meV in a region where some prominent Raman- and IR-active modes (Fig. 4) are activated by the folding of the acoustic branches [14,15]. The comparatively high sensitivity of HAS spectroscopy to CDW-induced phonons (which could not be seen with neutrons) was discussed in the pioneering work of Boato et al. [9], who in 1979 performed the first He diffraction study of TaS_2(001) in its $1T_3$ CDW phase. These authors showed that the satellite diffraction peaks associated with the CDW have about the same intensities as the Bragg peaks for the crystallographic cell. Consistently, a phonon displacement of the ions with a wavevector close to a CDW reciprocal g-vector will produce a relatively large dynamic modulation of the electronic charge density, which the He atoms can easily see. The observation by HAS of folded Rayleigh modes associated with different CDW g-vectors is an interesting physical effect. He atoms are inelastically scattered by the phonon-induced modulation of the surface electronic density, which means that Rayleigh phonons are able to modulate the part of the electronic density associated with the CDW. Thus we may speak of CDW–phonon coupled states. The signatures of such couplings are the gaps that should appear at the folding points.

This led us to an analysis of the data based on a tridimensional lattice dynamical calculation including the CDW–lattice coupling within the framework of the pseudocharge dynamical model [7]. In this model, besides the regular atomic

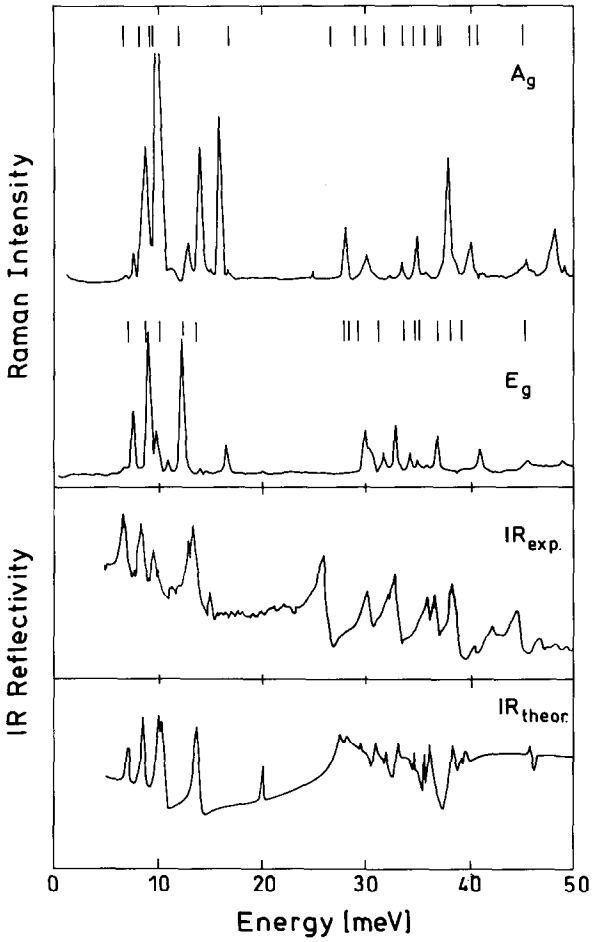

Fig. 4. *Top*: Experimental Raman scattering spectra for A_g and E_g modes (from Ref. [16]) compared with the calculated frequencies (vertical bars). *Bottom*: infrared reflectivity spectrum (from Ref. [15]) compared with the calculated reflection coefficient. All spectra are in arbitrary units.

lattice, one has a sublattice of pseudocharges suitably distributed in the $\sqrt{13} \times \sqrt{13}$ supercell in order to mimic the CDW distribution [10]. In the simplest version of the model six pseudocharges per unit ($\sqrt{13} \times \sqrt{13}$) cell, located around the Ta ions at each star of David centre (Fig. 1a), are coupled to the neighbouring metal and chalcogen ions through the radial force constants g_{bt} and g_{bs}, respectively. Moreover the simplest model requires a nearest-neighbour Ta–S radial force constant (f_{ts}) and two radial force constants between pairs of nearest-neighbour sulphur ions belonging to the same sandwich (f_{ss}) or to adjacent sandwiches ($f_{ss'}$). The force constants between metal ion pairs and between pseudocharge pairs are neglected and the few non-vanishing shear force constants of the model are fixed by the equilibrium conditions for the chosen pseudocharge configuration. Altogether, the model has five parameters and a certain arbitrariness in the choice of the location of the pseudocharges. Two configurations were considered: (a) the pseudoparticles are located in the metal plane at the centre of the triangles formed by three neighboring metal ions; and (b) the pseudoparticles are located at the centre of the flattened octahedron formed by three metal ions and three sulphur ions (PC in Fig. 1b). The calculations performed with the configuration (a) left many degeneracies unlifted and could not explain the complex distribution of Raman and IR which was instead reproduced with the configuration (b) used herein [10]. The model parameters were fitted to the zone-centre optical frequencies known from Raman scattering data [16] and infrared reflectance (IR) spectra [15] (Fig. 4). This model with only five parameters ($f_{ts} = 6.82$, $f_{ss} = 1.75$, $f_{ss'} = 0.702$, $g_{bt} = 15.70$ and $g_{bs} = 7.52$, all in 10^4 dyn/cm^{-2}) yields a fit of the 54 Raman and IR frequencies within a mean square relative deviation of 6%, as displayed in Fig. 4. The pseudocharge model, which implies a separation of the positive charge on Ta ions from the negative charge shared among S ions and the pseudocharges, also permits the calculation of the reflection coefficient; this is compared with the IR reflectivity spectrum in Fig. 4. The full set of dispersion curves (given in Ref. [10]) is rather complicated due to the extensive folding. Thus a comparison with the inelastic HAS data is conveniently made by plotting only the modes with large displacements of the sulphur ions normal to the layer. The ones best seen in HAS (dotted lines in Fig. 2, for $\Sigma_s |e_{z,s}|^2 > 8.014 \times 10^{-3}$ Å^{-2}, where e_s ($s = 1, 2, \ldots, 13$) are the displacements of the 13 sulphur ions on one single sheet of the unit cell). The HAS data clearly follow, along all three directions, the lowest lobes of the calculated phonon branches corresponding to different CDW g-vectors. Of

course, the lowest sets of measured points in the crystallographic directions may be viewed as belonging to a single, strongly anomalous transverse acoustic branch, the anomalies being the minima of the folded branches. Theory also predicts some intensity from a few flat branches above 10 meV, in agreement with the HAS observations. We conclude that the $1T_3$-TaS_2 transverse modes, which are approximately the Rayleigh waves, are strongly coupled to the CDW, whereas the ordinary electron–phonon interaction in most systems involves longitudinal phonons. These results provide another clear case illustrating the remarkable ability of HAS for studying the dynamics of strongly coupled electron–phonon systems.

Finally, we note that, unlike the $TaSe_2$ case [13], the HAS data on $TaS_2(001)$ did not show any peculiar surface phonon anomaly (besides the apparent anomalies due to folding), nor any deviation of the RW from the TA branch as known from neutron scattering, at least within the experimental errors. This may be surprising because the CDW–lattice coupling is supposedly larger in TaS_2 and the surface effects seen in $TaSe_2$ should be further emphasized in TaS_2. It must be noted, however, that all surface effects in $TaSe_2$ occur just around the CDW onset temperature T_c, whereas all HAS experiments on TaS_2 have been made much below T_c, in a region where the CDW is fully stabilized.

1. Acknowledgements

G.B. and P.R. acknowledge the financial support of the Alexander von Humboldt Stiftung, Germany. J.G.S. gratefully acknowledges support from the US Department of Energy under Grant No. DE-FG05-85ER45208 and NATO under Grant 891059.

2. References

[1] C.M. Varma, in: Charge Density Waves in Solids, Eds: H. Araki et al. (Springer, Berlin, 1985) p. 99;
C.M. Varma and A.L. Simons, Phys. Rev. Lett. 51 (1983) 138.

[2] K. Motizuki, Ed., Structural Phase Transitions in Layered Transition Metal Compounds (Reidel, Dordrecht, 1986);
R.L. Withers and J.A. Wilson, J. Phys. C (Solid State Phys.) 19 (1986) 4809.

[3] K.R.A. Ziebeck, B. Dorner, W.G. Stirling and R. Schöllhorn, J. Phys. F (Metal Phys.) 7 (1977) 1139.

[4] D.E. Moncton, J.D. Axe and F.J. di Salvo, Phys. Rev. B 14 (1977) 80.

[5] H. Bilz and W. Kress, Phonon Dispersion Relations in Insulators (Springer, Berlin, 1979).

[6] R. Brouwer and F. Jellinek, Physica B 99 (1980) 51.

[7] C. Kaden, P. Ruggerone, J.P. Toennies, G. Zhang and G. Benedek, Phys. Rev. B 46 (1992) 13509.

[8] C.B. Scruby, P.M. Williams and G.S. Parry, Philos. Mag. 31 (1975) 255.

[9] G. Boato, P. Cantini and R. Colella, Phys. Rev. Lett. 24 (1979) 1635.

[10] J.G. Skofronick and J.P. Toennies, in: Surface Properties of Layered Structures, Ed. G. Benedek (Kluwer, Dordrecht, 1992) ch. 4;
G. Benedek, F. Hofmann, P. Ruggerone, G. Onida and L. Miglio, Surf. Sci. Rep. 20 (1994) 1.

[11] C.G. Slough, W.W. McNairy, R.V. Coleman, J. Garnaes, C.B. Prater and P.K. Hansma, Phys. Rev. B 42 (1990) 9255.

[12] E. de Rouffignac, G.P. Alldredge and F.W. de Wette, Phys. Rev. B 23 (1981) 4208.

[13] G. Benedek, G. Brusdeylins, C. Heimlich, L. Miglio, J.G. Skofronick, J.P. Toennies and R. Vollmer, Phys. Rev. Lett. 60 (1988) 1037.

[14] J.R. Duffey and R.D. Kirby, Phys. Rev. B 23 (1981) 1534.

[15] D.R. Karecki and B.P. Clayman, Phys. Rev. B 19 (1979) 6367.

[16] S. Sugai, Phys. Status Solidi (b) 129 (1985) 13.